Supercontinuum Generation of Higher-Order Solitons by Fission in Photonic Crystal Fibers

A. V. Husakou and J. Herrmann*

Max Born Institute for Nonlinear Optics and Short Pulse Spectroscopy, Max-Born-Strasse 2a, D-12489 Berlin, Germany
(Received 22 March 2001; published 24 October 2001)

The nonlinear pulse propagation in photonic crystal fibers without slowly varying envelope approximation is studied using an improved variant of first-order wave equation. Supercontinuum generation is shown to be caused by a novel mechanism of spectral broadening through fission of higher-order solitons into redshifted fundamental solitons and blueshifted nonsolitonic radiation. Good agreement with experimental observations is found, and subcycle pulse compression is studied.

Microstructured photonic crystal fibers (PCFs) [1,2] have recently attracted significant attention because of their specifically controlled dispersion and waveguide properties, such as a shift of the zero-dispersion wavelength [3] into the visible range and single-mode operation over a large spectral range [2]. This lead to novel features in nonlinear processes such as the generation of an ultrabroadband continuum with a spectral width exceeding two octaves for relatively low intensities and long pulses, recently observed in PCF's [3] and tapered fibers [4]. Such a supercontinuum can be applied in different fields such as spectroscopy and pulse compression, and recently led to significant advance in frequency metrology and carrier phase stabilization [5,6]. Up to now, to our knowledge no theoretical exploration of pulse propagation in PCFs has yet been done.

In this Letter, we investigate the nonlinear propagation of femtosecond pulses in PCFs and find that in this system the pulse evolution shows new and surprising features which cannot be explained by the effect of self-phase modulation (SPM). We find that supercontinuum generation for relatively low intensities rests on a new mechanism of spectral broadening which is related to the evolution and fission of higher-order solitons near the zero-dispersion wavelength in PCFs. Because of higher-order dispersion, every emerging fundamental soliton emits a blueshifted nonsolitonic radiation phase matched to the soliton. Since the fundamental solitons have different central frequencies, the phase-matched radiation is generated at different frequency intervals which are extended up to the UV. For the description of these effects we derive a first-order equation for the electric field in forward propagation which is valid for arbitrary refractive indexes and is not restricted to the preconditions of the slowly varying envelope approximation (SVEA) and Taylor expansion for dispersion.

Pulse propagation without special prerequisites of the SVEA can be studied by the numerical solution of Maxwells equations with the use of the finite-difference time-domain method (see [7], and references therein). However, the large numerical effort in this approach limits the possible propagation lengths. With the neglect of back reflection and for a refractive index $n(\omega)$ close

to unity, the simpler so-called *reduced* Maxwell equation allows numerical solution for much longer propagation lengths [8,9]. In the following, we show that a more general first-order equation can be derived which is valid also for solids and liquids. The wave equation for the Fourier transformed field $\mathbf{E}(\mathbf{r}, \omega) = \int_{-\infty}^{\infty} e^{i\omega t} \mathbf{E}(\mathbf{r}, t) \, dt$, $\mathbf{r} = \{x, y, z\}$ is given by

$$\frac{\partial^2 \mathbf{E}(\mathbf{r}, \omega)}{\partial z^2} + k(\omega)^2 \mathbf{E}(\mathbf{r}, \omega) = - \Delta_\perp \mathbf{E}(\mathbf{r}, \omega) - \mu_0 \omega^2 \mathbf{P}_{NL}(\mathbf{r}, \omega), \quad (1)$$

where $\mathbf{E}(\mathbf{r}, t)$ is the electromagnetic field of a wave propagating in z direction, $k(\omega) = n(\omega)\omega/c$, $\mathbf{P}_{NL}(\mathbf{r}, \omega)$ is the Fourier transform of the nolinear polarization.

Now we use the formal relation $\partial^2/\partial z^2 + k(\omega)^2 = [\partial/\partial z - ik(\omega)][\partial/\partial z + ik(\omega)]$ and neglect back reflection, which leads to the approximation $\partial \mathbf{E}(\mathbf{r}, \omega)/\partial z \simeq -ik(\omega)\mathbf{E}(\mathbf{r}, \omega)$. With the introduction of the moving time coordinates $\xi = z, \eta = t - z/c$
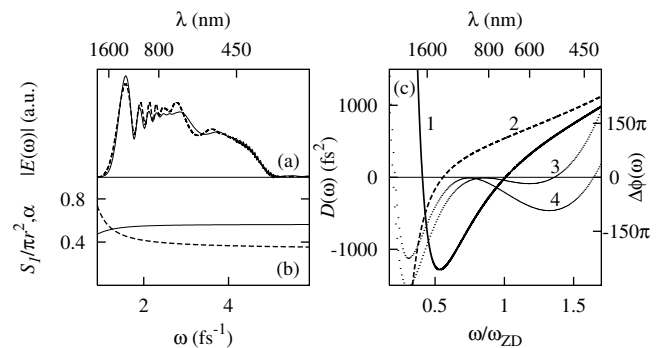

FIG. 1. Pulse spectra calculated by different propagation equations (a) and PCF parameters (b),(c). Spectra of a 40-TW/cm², 15-fs pulse after propagating 0.5 mm of a standard fiber calculated by full Maxwell equations (dashed), and FME (solid) are presented (a). Nonlinear reduction factor $\alpha(\omega)$ (solid) and effective mode area S_1 (dashed) are shown in (b). GVD parameters for PCF with $\Lambda = 1.5 \ \mu$m, $d = 1.3 \ \mu$m (curve 1), and bulk silica (curve 2) together with phase mismatch between radiation at frequency ω and solitons with central frequencies of $0.85\omega_{ZD}$ (curve 3) and $0.74\omega_{ZD}$ (curve 4) are shown in (c).

with $\partial/\partial z = \partial/\partial\xi - c^{-1}\partial/\partial\eta$, we obtain the following basic equation in Fourier presentation which we denote in the following as forward Maxwell equation (FME):

$$\frac{\partial \mathbf{E}(\mathbf{r}, \omega)}{\partial\xi} = i\,\frac{[n(\omega) - 1]\omega}{c}\,\mathbf{E}(\mathbf{r}, \omega)$$
$$+ \frac{i}{2k(\omega)}\Delta_\perp \mathbf{E}(\mathbf{r}, \omega) + \frac{i\mu_0\omega c}{2n(\omega)}\mathbf{P}_{NL}(\mathbf{r}, \omega). \tag{2}$$

For linearly polarized waves $\mathbf{P}_{NL,x} = \epsilon_0\chi_3 E_x^3$, the frequency dependence of χ_3 is negligible for wide-gap solids [10] as well as the Raman process (proved by numerical calculation). Equation (2) can be numerically solved by the second-order split-step Fourier method with fourth-order Runge-Kutta nonlinear steps. For a check of the validity of this equation, in Fig. 1(a) the numerical solutions for the exact wave equation (1) (dashed, taken from Ref. [7]), and the FME (2) (solid) are presented for propagation in standard fibers made of fused silica in a parameter range where the SVEA is not valid. Comparison shows that the deviation is negligible in the whole spectral range, in contrast to the solution of reduced Maxwell equation (not shown here). The energy transfer to higher modes is weak, and the electric field in frequency domain can be separated in the form: $\mathbf{E}(x, y, z, \omega) = \mathbf{F}(x, y, \omega)\tilde{E}(z, \omega)$, where the transverse fundamental mode distribution $\mathbf{F}(x, y, \omega)$ is the solution of the Helmholtz equation $\Delta_\perp\mathbf{F} + k(\omega)^2\mathbf{F} = \beta(\omega)^2\mathbf{F}$ for a PCF with the eigenvalue $\beta(\omega)$. To determine $\beta(\omega)$, we calculate the effective refractive index $n_{\text{eff}}(\omega)$ for the fundamental mode in the photonic crystal, as done in Ref. [2]. Then we consider the omitted hole as a core of a step-index fiber with diameter $2r = 2\Lambda - d$, where Λ is the center-to-center distance between the holes (pitch) and d is the hole diameter, and the surrounding photonic crystal as homogeneous cladding with refractive index $n_{\text{eff}}(\omega)$. The longitudinal distribution $\tilde{E}(\xi, \omega)$ satisfies an equation analogous to Eq. (2) with the substitutions $n(\omega)\omega/c \rightarrow \beta(\omega)$, $\chi_3 \rightarrow \alpha(\omega)\chi_3$ and without the $\Delta_\perp$-term. Here $\alpha(\omega) = \int_S F^4(x, y, \omega)\,dS/S_1 \approx 0.55$ is a nonlinearity reduction factor depicted in Fig. 1(b) together with the effective mode area $S_1(\omega) = \int_S F^2(x, y, \omega)\,dS \approx 0.4\pi r^2$.

The GVD parameter $D = L\partial^2\beta(\omega)/\partial\omega^2$ calculated by the use of this model for a propagation length $L = 15$ mm is presented in Fig. 1(c) by curve 1 for PCF and by curve 2 for bulk silica. The dispersion is anomalous in the range from 710 to 1700 nm and the relatively large third-order dispersion (TOD) parameter is positive. The calculated dispersion is in good agreement with corresponding measurements [3].

First we study pulse propagation in a PCF with $\Lambda = 1.5\ \mu$m, $d = 1.3\ \mu$m, and the zero dispersion frequency $\omega_{\text{ZD}} = 2.66$ fs^{-1} ($\lambda_{\text{ZD}} = 710$ nm) for pulses with large duration (FWHM) $\tau_0 = 100$ fs, a relatively low intensity $I_0 = \epsilon_0 n(\omega)cE^2/2 = P_0/S_1 = 0.6$ TW/cm^2, and initial central frequency $\omega_0 = 0.85\omega_{\text{ZD}}$ (initial wavelength $\lambda_0 =$

830 nm). After about 10 mm the spectrum is seen to broaden significantly with a larger extension into the violet and a width of more than 500 nm. The theoretical prediction presented in Fig. 2(b) is in good agreement with experimental measurements for the same input pulse parameters reported in Ref. [3]. The evolution of the temporal shape presented in Fig. 2(a) shows that the pulse is successively split into up to finally seven ultrashort peaks moving with different velocities with shapes which do not change their form over a long distance. It is impossible to explain the extremely broad spectrum for the rather long pulses with a relatively small intensity by the effect of SPM. The largest spectral broadening by SPM is given (if the influence of dispersion can be neglected) by [11] $\Delta\omega_{\text{SPM}}/\omega_0 = 1.39n_2I_0L/(\tau_0 c) = 0.07$ for the input pulse parameters in Fig. 2, while in Fig. 2, we obtained a more than 1 order of magnitude broader spectrum. Here $n_2 = 3\chi_3/[4\epsilon_0 cn^2(\omega)] = 3 \times 10^{-4}$ cm^2/TW is the nonlinear refractive index of silica. Additionally, we find a surprising result if we consider the spectral broadening of a shorter pulse with the same intensity, as shown in Fig. 3. As can be seen in Fig. 3, for $\omega_0 = 0.85\omega_{\text{ZD}}$ the spectral width of about 50 nm generated by a 17.5 fs pulse is ten times smaller compared with the 100-fs-pulse case in Fig. 2. This much narrower spectrum is in direct contrast to the behavior of SPM-induced broadening, where, corresponding the relation for $\Delta\omega_{\text{SPM}}/\omega_0$, an about 6 times shorter pulse should yield a correspondingly larger width. The temporal shape presented in Fig. 3 (top) shows the formation of a single short spike together with background radiation. While the spike does not change its form during propagation from 15 to 75 mm, the background radiation becomes temporally broadened.

The behavior of supercontinuum generation in PCFs described above is qualitatively different from SPM-induced broadening and requires a careful study of its physical origin. Note that the considered input frequency $0.85\omega_{\text{ZD}}$ in Figs. 2 and 3 is in the anomalous region and, therefore, soliton dynamics plays a crucial role in the propagation.
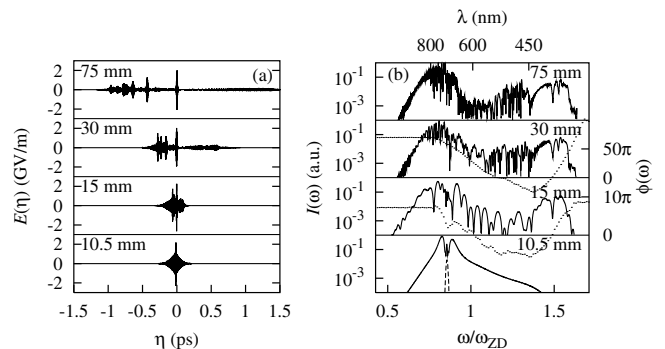

FIG. 2. Evolution of pulse shape (a) and spectrum (b) for $\tau_0 = 100$ fs, $I_0 = 0.6$ TW/cm^2 in PCF with $\Lambda = 1.5\ \mu$m, $d = 1.3\ \mu$m. Spectral phases (dotted) and initial spectrum (dashed, scaled for clarity here and hereafter) are also presented.
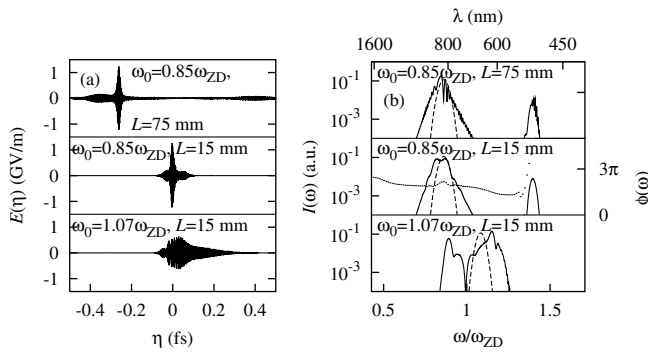
FIG. 3. Output pulse shapes (a) and spectra (b) for $I_0 = 0.6$ TW/cm^2, $\tau_0 = 17.5$ fs for different initial frequencies and propagation length as indicated. Spectral phase (dotted) are also presented.

The input parameters in Fig. 2 imply the formation of a higher-order soliton [11] with a soliton number $N = \sqrt{n_2 I_0 \omega_0 \tau_0^2 L / |D| c} = 7.8$. Higher-order solitons of the nonlinear Schrödinger equation (NSE) show periodic changes with propagation and cannot explain the effects described above. But here the input wavelength is in the vicinity of the zero-dispersion wavelength with strong influence of TOD. Previous studies [12–15] of the perturbed NSE, taking into account positive TOD and the self-steepening effect, predict the following behavior: A higher-order soliton with number N splits into N pulses with different redshifted central frequencies and different group velocities [12]. After the fission every pulse emits nonsolitonic radiation phase matched to the corresponding pulse [14,15] while simultaneously moving to IR until the stability is reached [15]. Although the perturbed NSE is not valid for the propagation phenomena illustrated by Fig. 2 and the spectral broadening and shifts in standard fibers are 2 orders of magnitude smaller, the analogous effects in PCFs can be readily identified as the physical origin of the supercontinuum generation. The amplitudes and durations of the separated spikes in Fig. 2(a) satisfy the relation for a fundamental soliton [11]. To corroborate the soliton nature of these spikes, we simulate the propagation of every separated pulse over a distance of 75 mm and do not find any change in shape and spectrum during propagation. For the same conditions a low-intense pulse would spread by a factor of 200. All spectral components of each soliton are phase locked and the solitons preserve their shape and spectrum in collisions. The calculated spectrum of the three isolated strongest solitons shows a redshift with central frequencies at $0.87\omega_0$, $0.93\omega_0$, and $0.97\omega_0$, and its velocities are close to corresponding group velocities. The phases of a soliton at frequency ω_s and that of the nonsolitonic radiation at ω are given by $\phi_s(\omega_s) = n(\omega_s)\omega_s L/c + n_2 I \omega_s L/(2c) - \omega_s L/v_s$ and $\phi_r(\omega) = n(\omega)\omega L/c - \omega L/v_s$, correspondingly. In Fig. 1(c) in curves 3 and 4 the phase difference $\Delta\phi = \phi_s - \phi_r$ for the strongest and weakest soliton

with respect to its corresponding nonsolitonic radiation is presented. The strongest soliton is phase matched with nonsolitonic radiation at 400 nm and the weakest at 550 nm. Because of the presence of several solitons with different frequencies, distinct spectral fractions arise and therefore a broad spectrum is generated in the intermediate range between 430 to 550 nm. The spectrum in the range between 550 and 700 nm arises as a result of four-wave mixing between the solitons and the blueshifted continuum. The phase relations discussed above are supported by the numerically calculated spectral phases of the pulses $\tilde{\phi}$. In the dotted lines in Fig. 2 the modified phase $\tilde{\phi}(\omega) = \phi(\omega) - \omega L(1/v_s - 1/c)$ is plotted. As can be seen the blueshifted part of radiation with highest frequencies is indeed phase matched with the most intense fundamental soliton, and analogous phase relations can be found for the other solitons. Now the unexpected result in Fig. 3 for a shorter input pulse but a narrower output spectrum can be clearly explained. Since for the smaller pulse duration the soliton number with $N = 1.5$ corresponds to one fundamental soliton, no soliton fission can occur and only an isolated blueshifted side peak is generated. Additionally, we consider in the lowest section of Fig. 3 the propagation of a pulse with the same parameters but different initial frequency $\omega_0 = 1.07\omega_{ZD}$. Here we see typical splitting behavior around the zero-dispersion point similarly as previously found in Ref. [13].

In order to study the crucial role of the specific PCF dispersion, we consider the propagation of pulses with different initial frequencies presented in Fig. 4. For the parameters in Fig. 4 with an initial frequency $\omega_0 = 0.6\omega_{ZD}$ the soliton number is $N = 4.3$ and, differently from the previous cases, the magnitude of the negative GVD parameter D is larger and the TOD parameter is very small. Therefore in this case SVEA and the prediction of the NSE should be valid. Indeed the solution presented in Fig. 4 for $\omega = 0.6\omega_{ZD}$ can be identified as a bounded fourth-order soliton of NSE with typical periodic evolution with the propagation length and splitting into three distinct peaks which merge again later [11]. At initial frequency $\omega_0 = 1.37\omega_{ZD}$ in normal dispersion range, spectral broadening typical for SPM can be found, with a spectral width
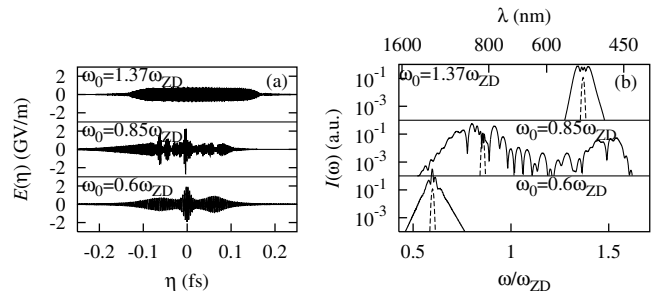

FIG. 4. Output pulse shapes (a) and spectra (b) for $L = 15$ mm, $I_0 = 0.6$ TW/cm^2, $\tau_0 = 100$ fs and different initial frequencies as indicated.
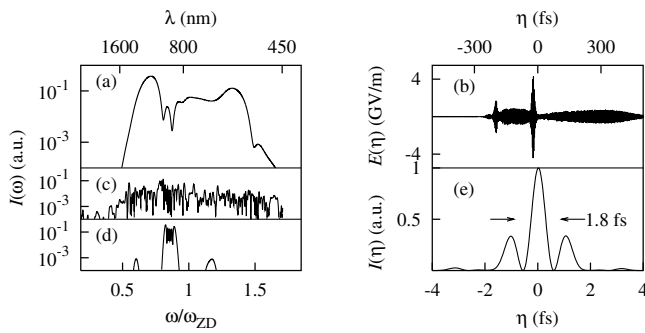
FIG. 5. Output characteristics for a higher input intensity $I = 3.3$ TW/cm^2 and for $\omega_0 = 0.92\omega_{ZD}$. For short 10-fs pulses the spectrum (a) and the temporal shape (b) are presented, demonstrating the supercontinuum generation by soliton fission. The evolution of spectrum in (d),(c) for 200-fs pulse shows the influence of four-wave mixing on spectral broadening. Section (e) exemplifies subcycle pulse compression by a LC SLM. Propagation length L is 1.5 mm (a), 15 mm (b), 9 mm (c), 4.5 mm (d), and 9 mm (e).

more than 1 order of magnitude smaller than that observed for higher-order-soliton fission for $\omega_0 = 0.85\omega_{ZD}$ (Fig. 4).

Finally, we demonstrate in Figs. 5(a) and 5(b) that for a 10-fs pulse, but with 5.5 times higher input intensity in a photonic fiber with $\Lambda = 1.65$ μm and $d = 1.3$ μm (corresponding $\lambda_{ZD} = 767$ nm and $N = 2.87$) soliton fission also can produce supercontinua. The temporal shape (b) demonstrates fission into two solitons with their blueshifted emission as the reason for supercontinuum generation in Fig. 5(a). The spectrum covers the range 500–1300 nm and agrees with the recent experimental observations [6] for the same parameters. For a longer 200-fs pulse with the same higher intensity, besides soliton fission spectral broadening by four-wave mixing play role: First, side peaks emerge at frequencies determined by four-wave mixing phase-matching condition [Fig. 5(d)], and then supercontinuum arises as a result of interaction between the distinct spectral parts [Fig. 5(c)]. In the normal GVD regime and for short and intense pulses, SPM is the only reason for ultrawide spectral broadening.

Ultrawide spectra, such as in Fig. 5(c), can be used to produce extremely short pulses if the spectral phase is compensated. Here we consider a liquid crystal spatial light modulator (LCSLM) (see, e.g., [7,9] and references therein). After the LCSLM a subcycle pulse [Fig. 5(e)] is generated with a duration of 1.8 fs determined from fitted Gaussian envelope and 0.6 fs FWHM.

In conclusion, it is shown that supercontinuum in PCF's by relatively long and low-intense pulses does not rely on SPM but is caused by a novel mechanism of spectral broadening due to fission of higher-order solitons.

*Email address: jherrman@mbi-berlin.de

[1] J. C. Knight *et al.,* Opt. Lett. **21**, 1547 (1996).
[2] T. A. Birks, J. C. Knight, and P. St. J. Russel, Opt. Lett. **22**, 961 (1997).
[3] J. K. Ranka, R. S. Windeler, and A. J. Steinz, Opt. Lett. **25**, 25 (2000).
[4] T. A. Birks, W. J. Wadsworth, and P. St. J. Russel, Opt. Lett. **25**, 1415 (2000).
[5] R. Holzwarth *et al.,* Phys. Rev. Lett. **85**, 2264 (2000).
[6] D. A. Jones *et al.,* Science **288**, 635 (2000).
[7] V. P. Kalosha and J. Herrmann, Phys. Rev. A **62**, 011 804(R) (2000).
[8] V. P. Kalosha and J. Herrmann, Phys. Rev. Lett. **85**, 1226 (2000); Opt. Lett. **26**, 456 (2001).
[9] A. V. Husakou, V. P. Kalosha, and J. Herrmann, Opt. Lett. **26**, 1022 (2001).
[10] M. Sheik-Bahae *et al.,* J. Quantum Electron. **27**, 1296 (1991).
[11] G. P. Agrawal, *Nonlinear Fiber Optics* (Academic Press, New York, 1994).
[12] Y. Kodama and A. Hasegawa, IEEE J. Quantum Electron. **23**, 510 (1987).
[13] P. K. A. Wai *et al.,* Opt. Lett. **12**, 628 (1987).
[14] J. N. Elgin, T. Brabec, and S. M. J. Kelly, Opt. Commun. **114**, 321 (1995).
[15] N. Akhmediev and M. Karlsson, Phys. Rev. A **51**, 2602 (1995).